The LNLS dispersive XAS (DXAS) beam line

Gustavo Azevedo

Edson Carvalho

Flavio Garcia*

X-ray Absorption Spectroscopy

Laboratório Nacional de Luz Síncrotron

Outline

- LNLS overview
- DXAS beam line
- Examples

LNLS- National Synchrotron Light Laboratory

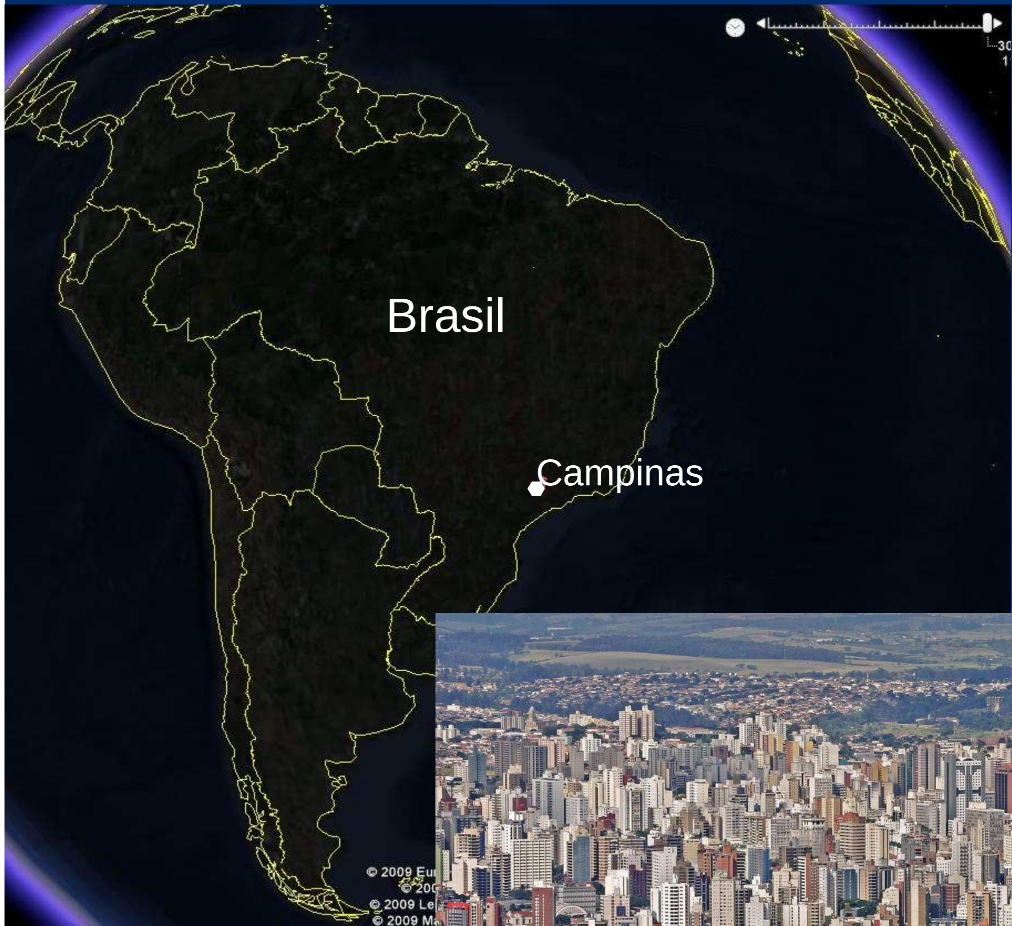

Operated by **ABTLuS:**
***A**ssociação **B**rasileira de **T**ecnologia de **L**uz **S**íncrotron,*
under contract with the Brazilian Ministry of Science and Technology

Population:3 Million
Economy: Agriculture, Industry, Services (3% of national GNP)
Several Universities, Colleges and Research Institutes (10% of national scientific production)

LNLS Campus

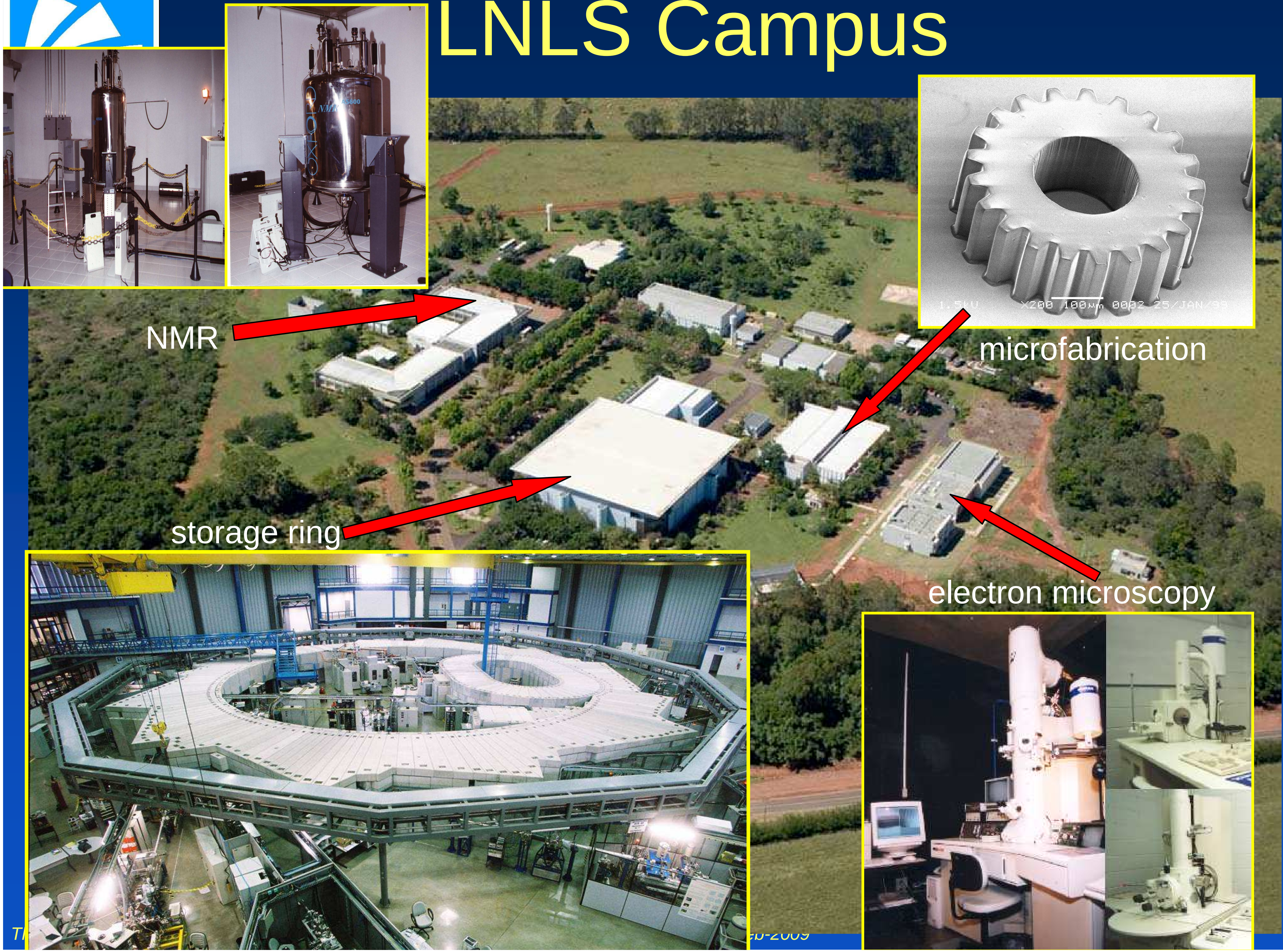

Open, multi-disciplinary and multi-user infrastructure for research at the LNLS

- **synchrotron light source**
- **molecular biology**
- **protein crystallization**
- **NMR spectroscopy**
- **mass spectrometry**
- **electron microscopy**
- **scanning probe microscopy**
- **mechanical microfabrication**
- **chemical syntesis laboratory**
- **engineering (scientific instrumentation)**

Light source layout and parameters

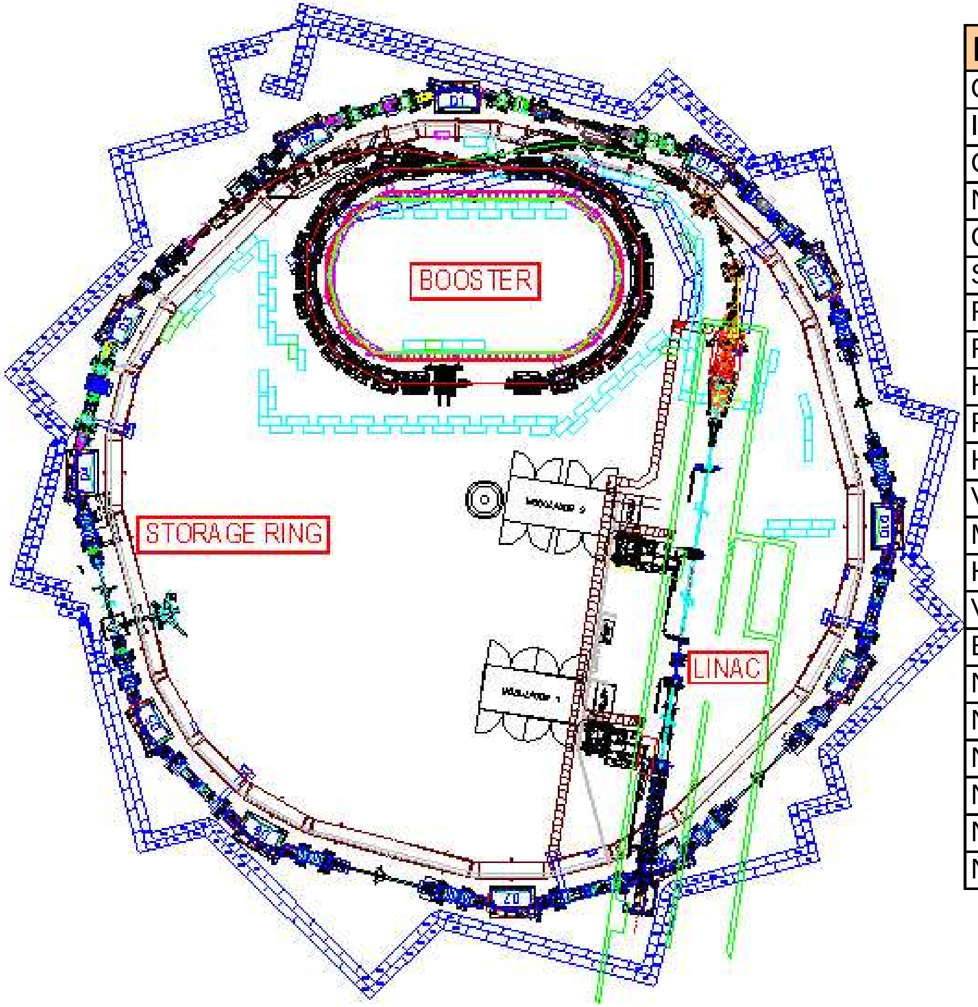

LNLS UVX2 Parameters		
Operating energy	1.37	GeV
Injection energy	500	MeV
Critical photon energy	2.08	keV
Natural emittance	100	nm rad
Circumference	93.2	m
Straight section free length	2.95	m
Revolution frequency	3.22	MHz
Revolution period	311	ns
Harmonic number	148	
RF frequency	476	MHz
Horizontal tune	5.27	
Vertical tune	2.17	
Momentum compaction factor	0.0083	
Horizontal natural chromaticity	-7.8	
Vertical natural chromaticity	-9.5	
Energy loss per turn	114	keV
Number of dipoles	12	
Number of quadrupoles	36	
Number of sextupoles	18	
Number of horizontal correctors	18	
Number of vertical correctors	12	
Number of BPMs	24	

Beam lines

VUV/Soft X-rays

•3 in operation

•1 comissioning

•1 in construction

Hard X-rays

•11 em operação

•1 comissioning.

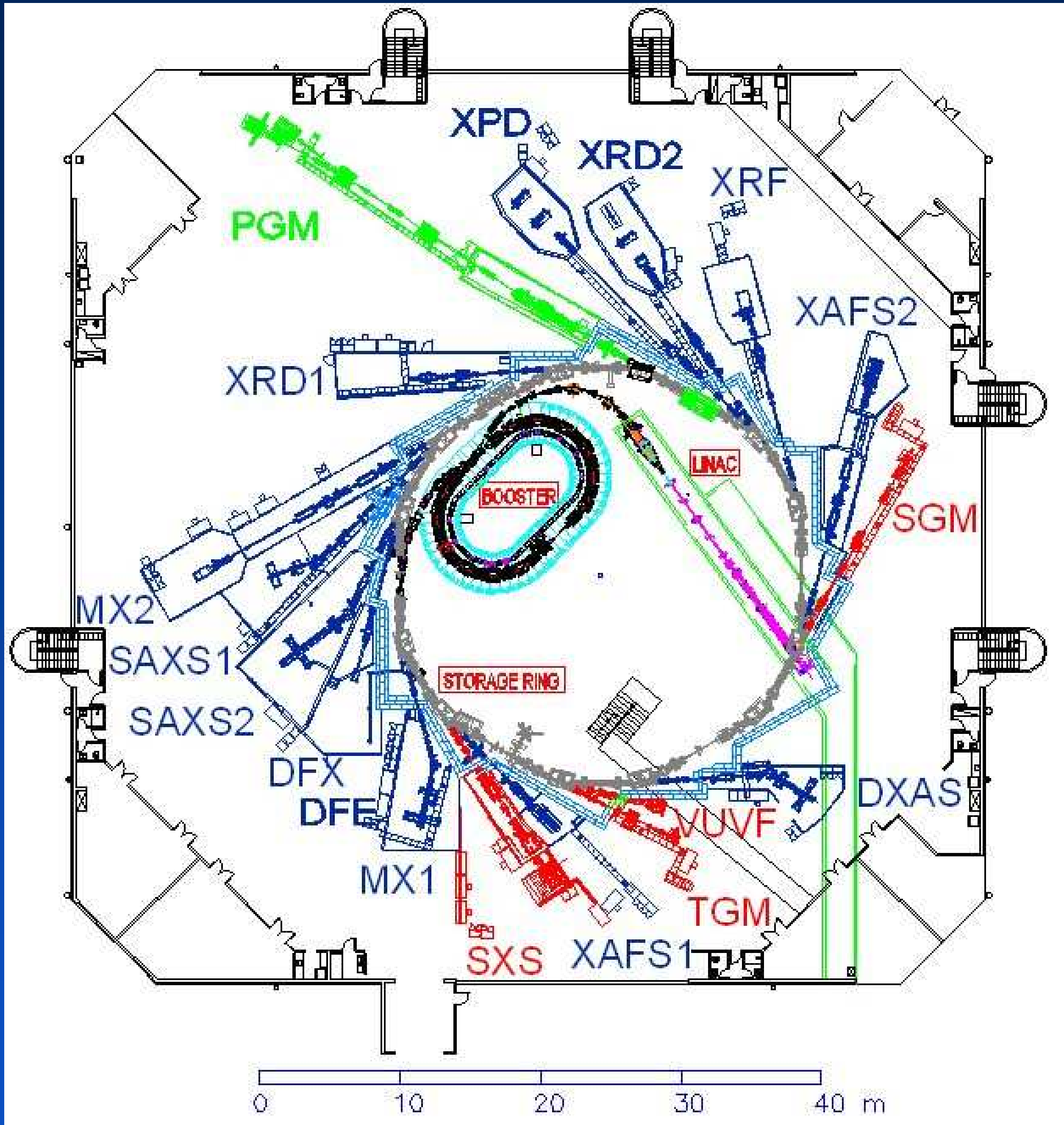

DXAS Layout

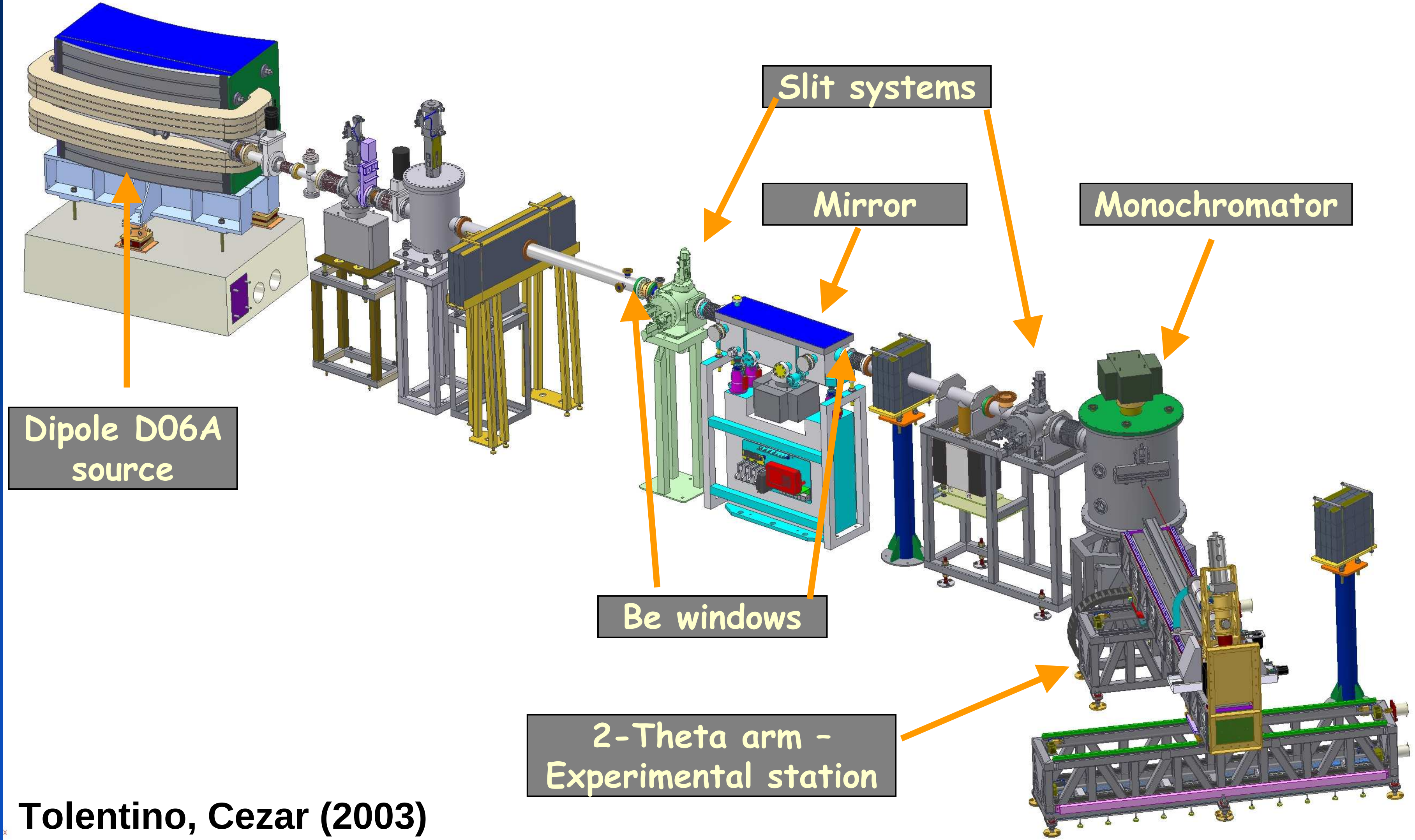

Tolentino, Cezar (2003)

DXAS Layout

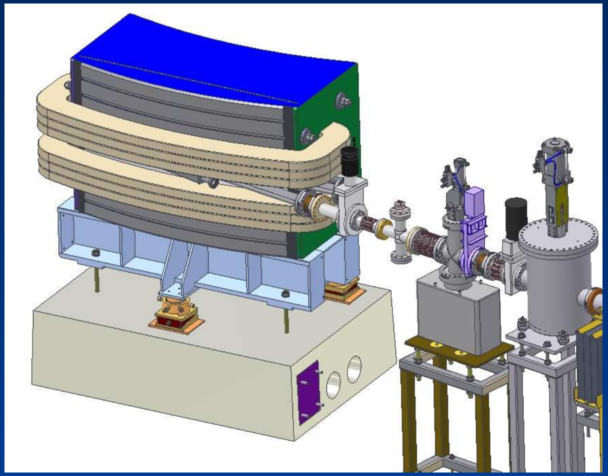

X- Ray Source
Bending Magnet (BM)
Beam Size (Source): 0.25mm (V) $\times$ 0.89mm (H)
BM/Monochromator distance = 9.75m

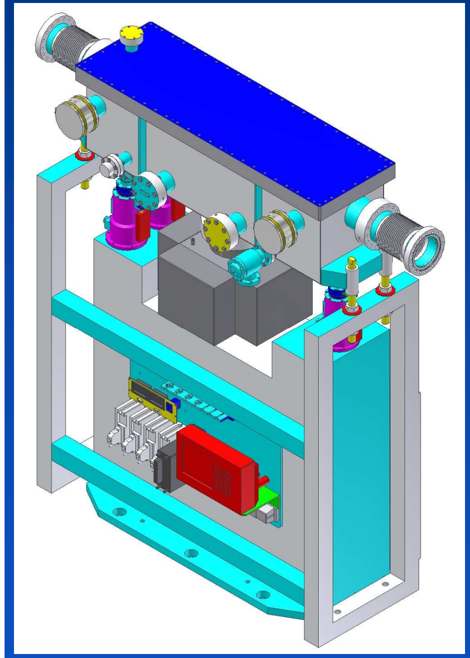

Mirror
800mm-long Rh coated mirror
Bending mechanism $\Rightarrow$ vertical focused beam $\approx$ 500µm

Slits
Two sets of water-cooled slits

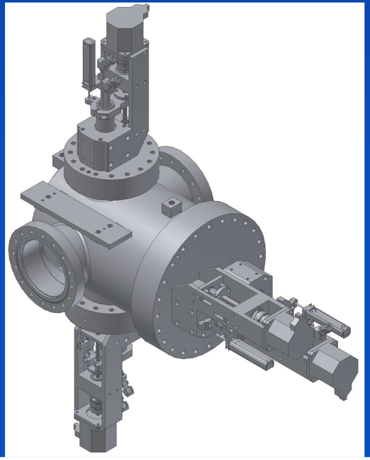

Monochromator

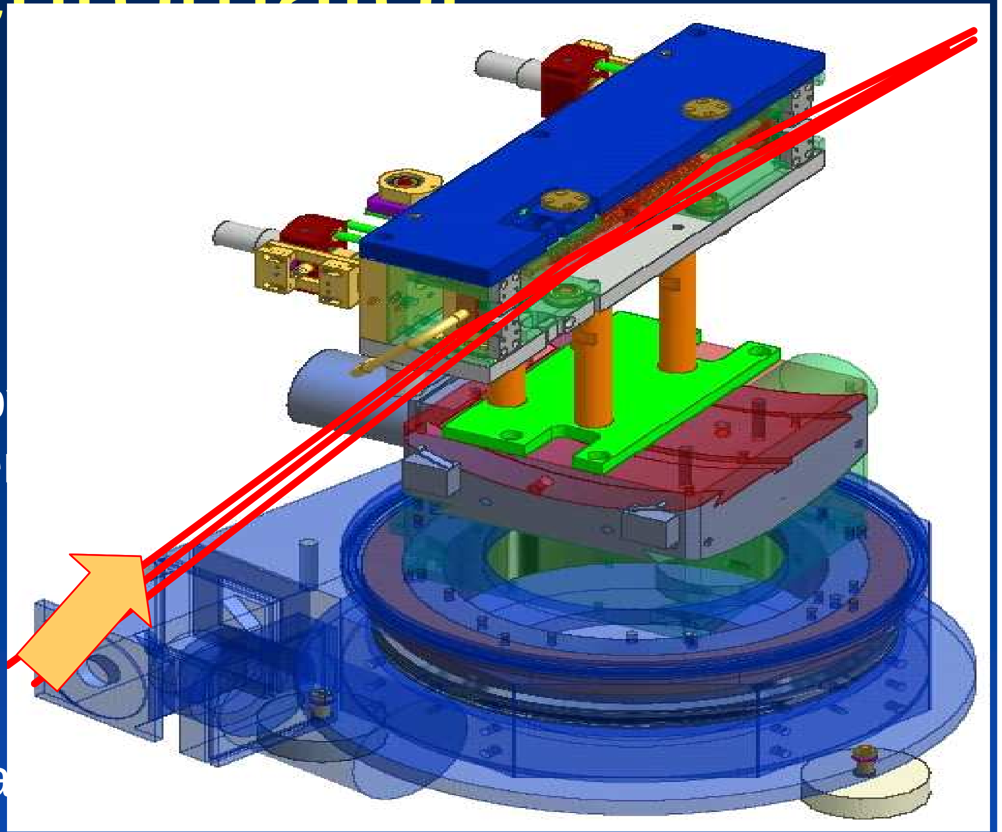

Si <111> Crystal

Bending mechanism:

LNLS Design – curvature is imposed b
independent momenta on crystal extre

All other rotations – High precision
Huber goniometers

Typical vertical size of the focused bea

Energy Range – 4 keV to 14 keV

Main Absorption edges
- **K** – Ti, Cr, Mn, Co, Ni, Ge, Fe, Cu, Ga
- **L** – Pt, Au, Re, La, TR

Detector

Cryogenically cooled CCD (1300 ×1340 pixels), each pixel⇒20×20μm

GdOS Phosphor screen, optimized for 8KeV ⇒ conversion of the x-ray photons in visible photons

Lens set ⇒ project the phosphor screen image on the CCD with a demagnification factor of 1.75

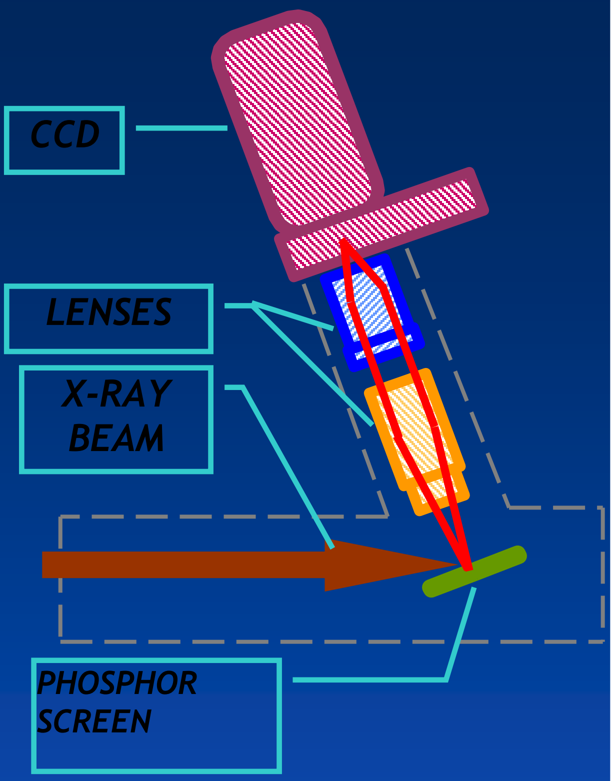

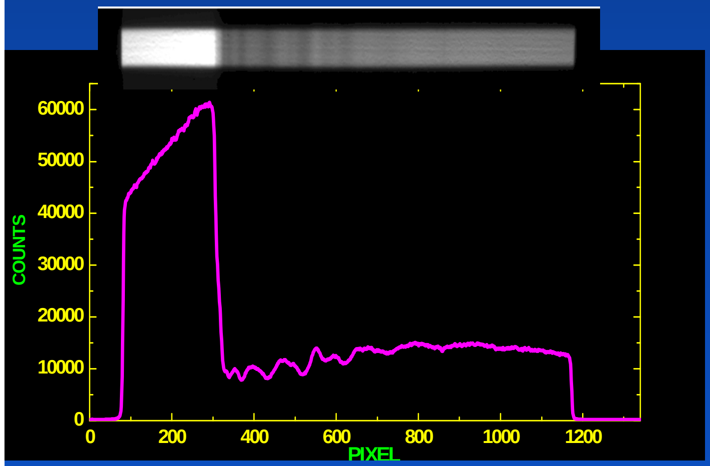

Data acquisition: image or spectroscopy mode

Minimal acquisition time: 1ms

Typical readout time: 20ms

Experimental station

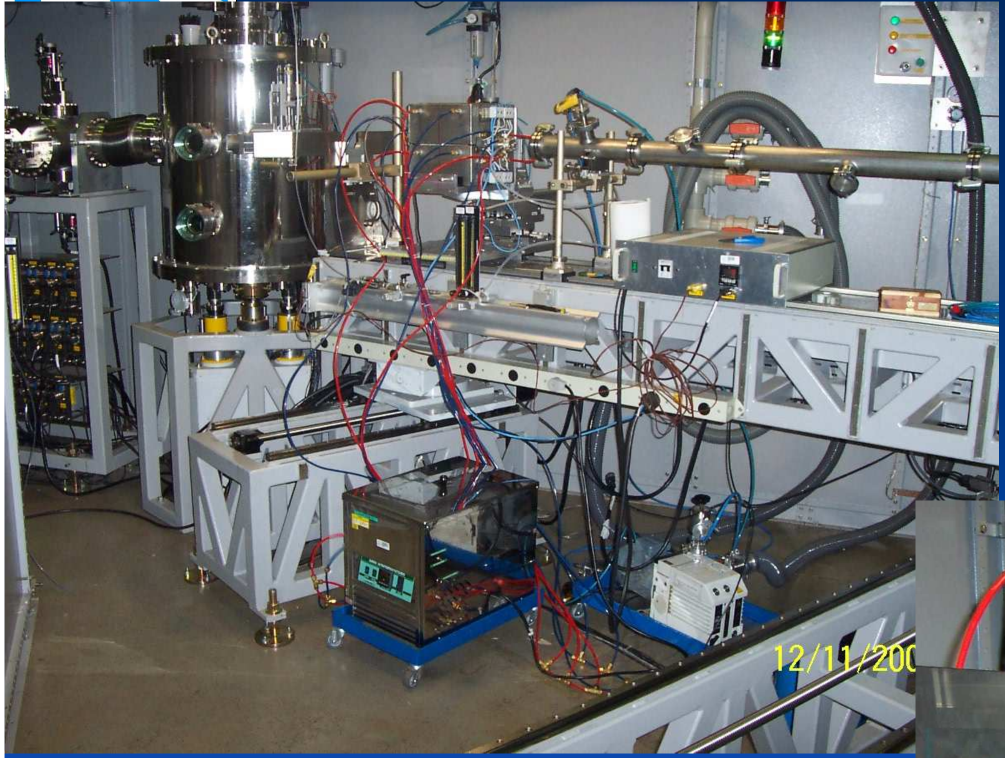

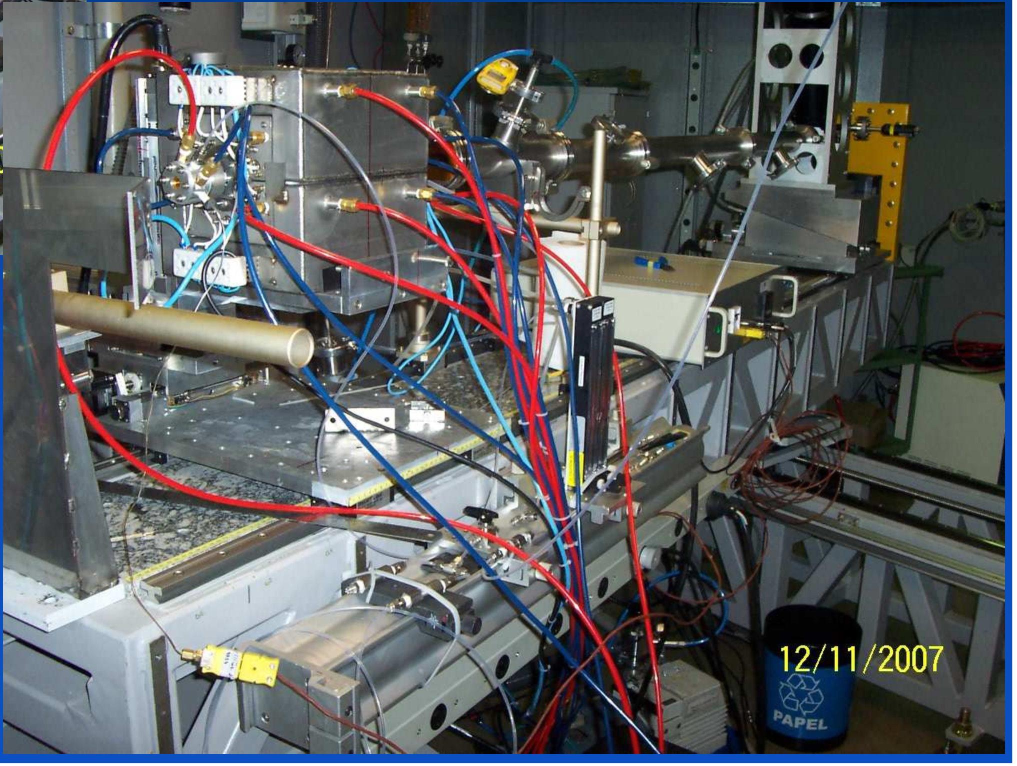

Beam line Parameters

Dispersive optics

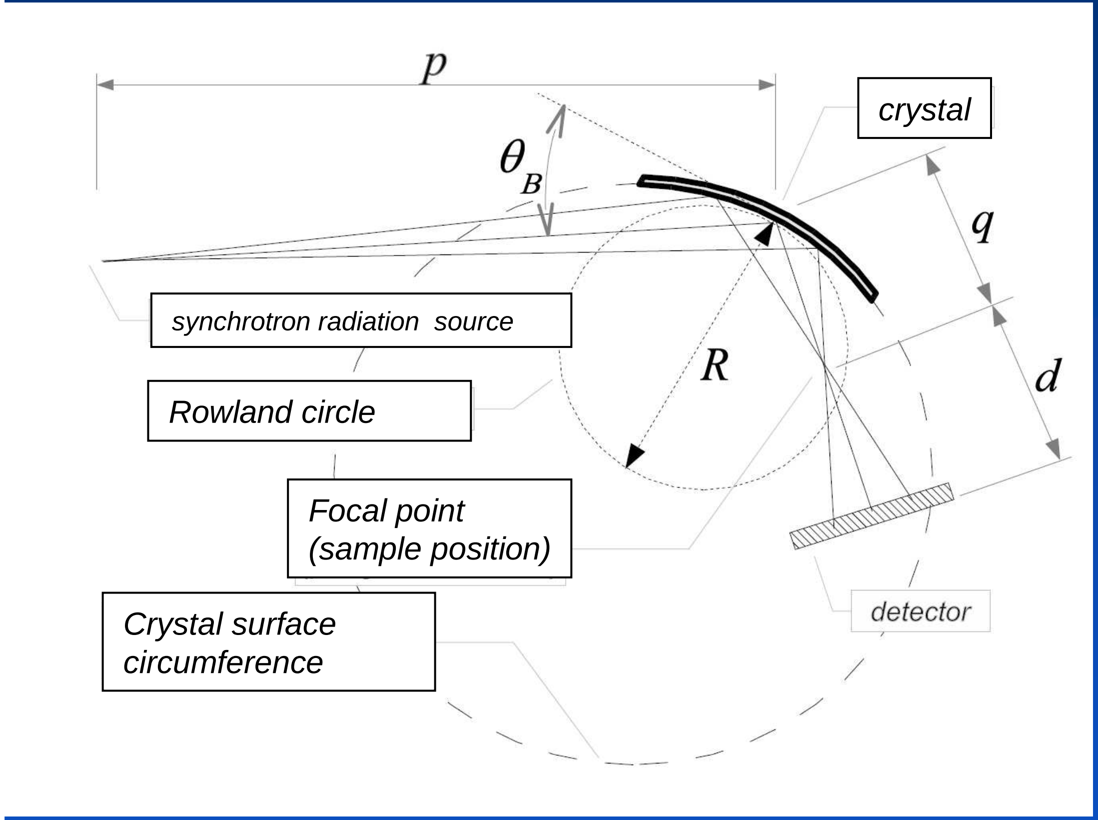

Energy bandwidth

$$\Delta E = E\cot\theta_B\left[\frac{L}{R} - \frac{L\sin\theta_B}{p}\right]$$

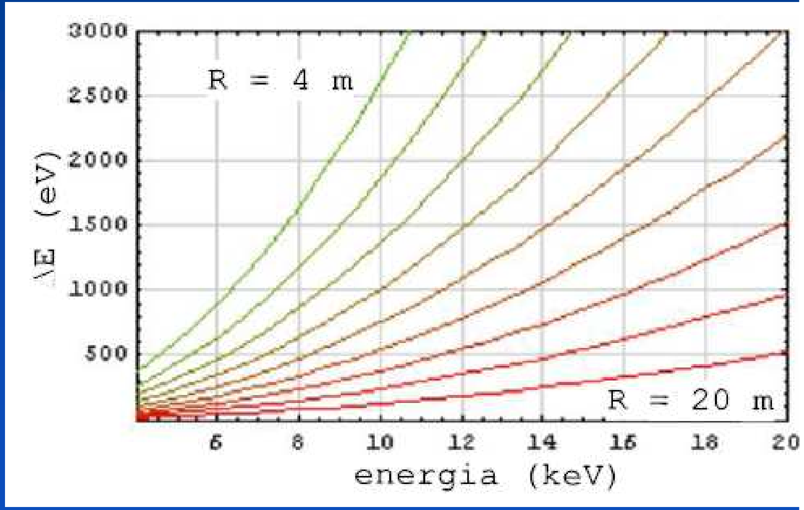

J. C. Cezar, PhD. Thesis – UNICAMP 2003

Energy resolution

$$\delta E = E \cot\theta \delta\theta$$

Main contributing terms:

- CCD pixel width: $\delta\theta_1$
- Source size: $\delta\theta_2$
- Darwin width: Ω_D

$$\delta\theta = \sqrt{\delta\theta_1^{\ 2} + \delta\theta_2^{\ 2} + \Omega_D^2}$$

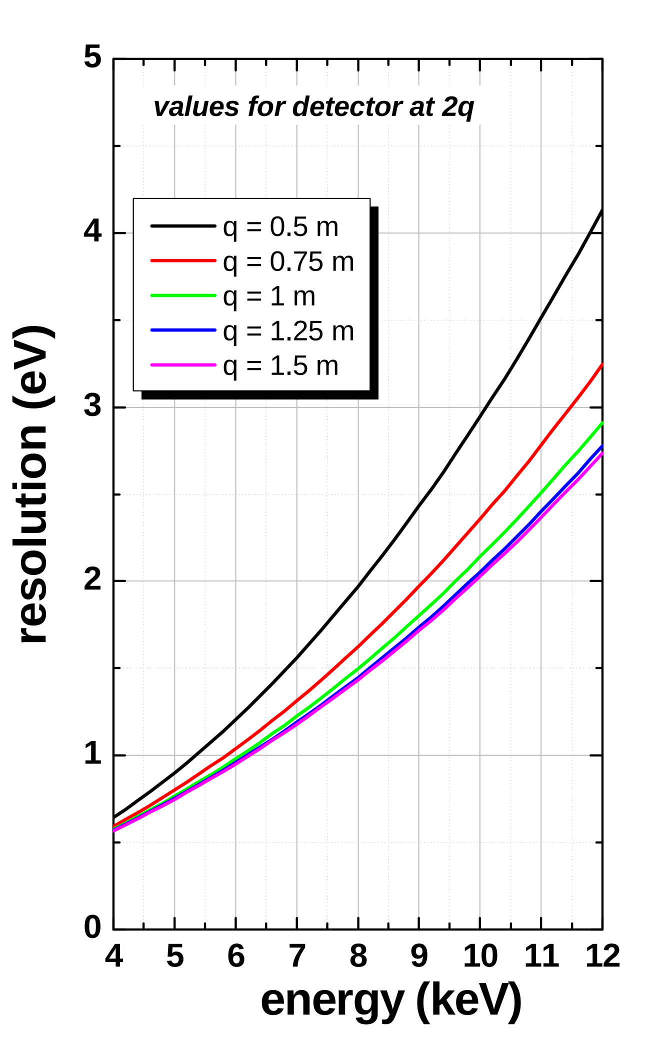

Flux

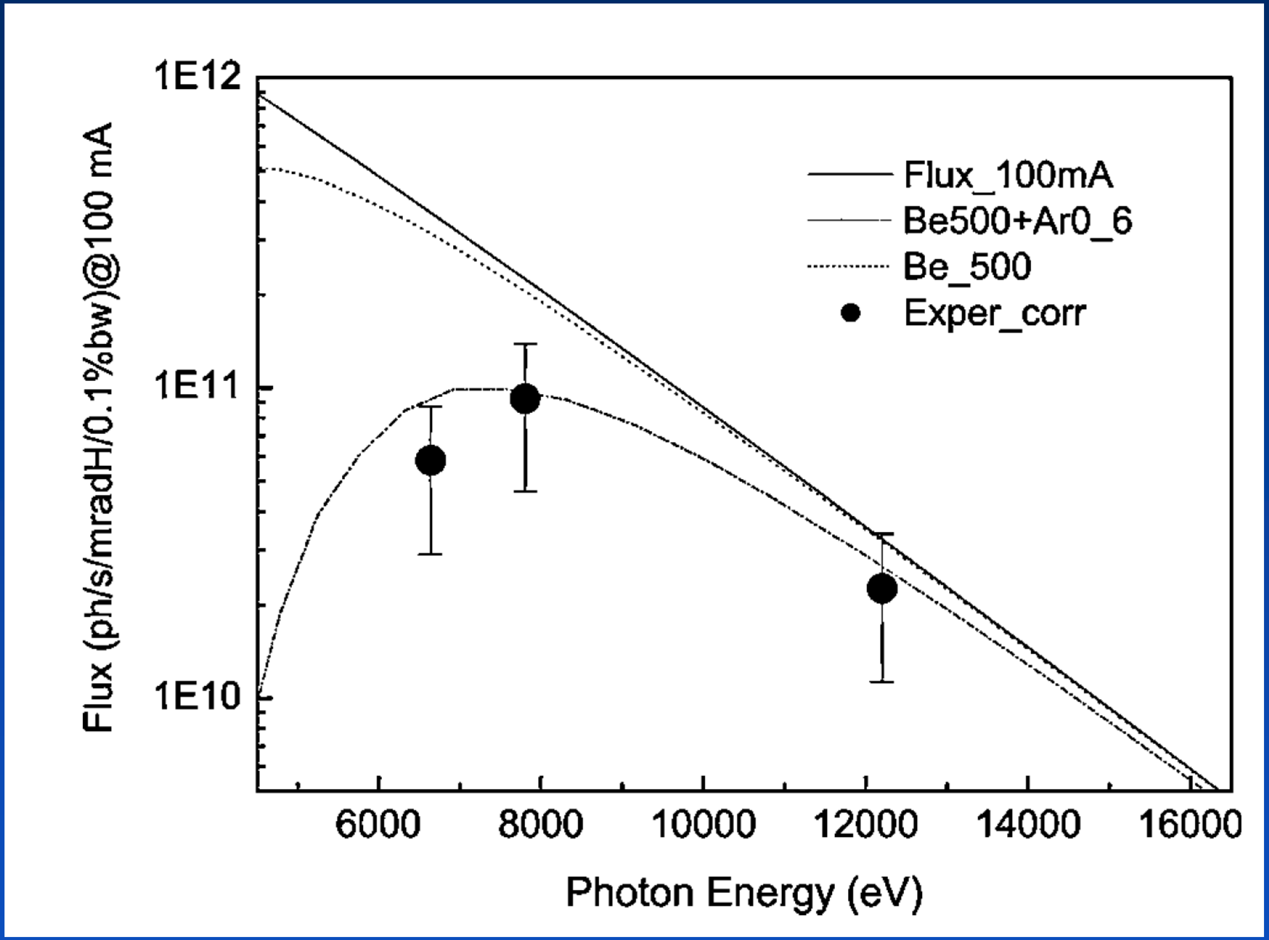

Tolentino et al, Phys. Scr. **T115**, 977 (2005)

Copper K edge- DXAS beam line - July 24, 2002

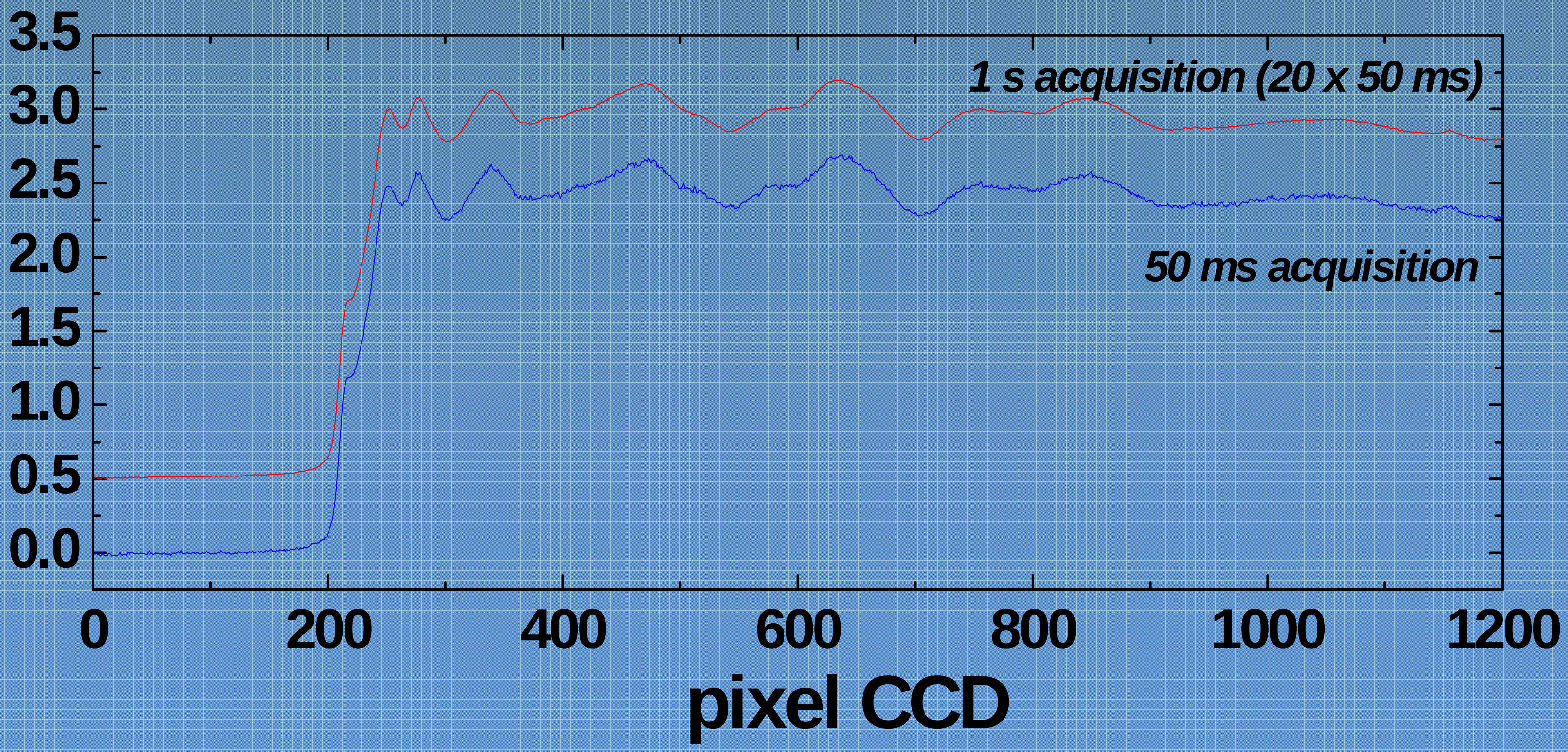

Scientific areas

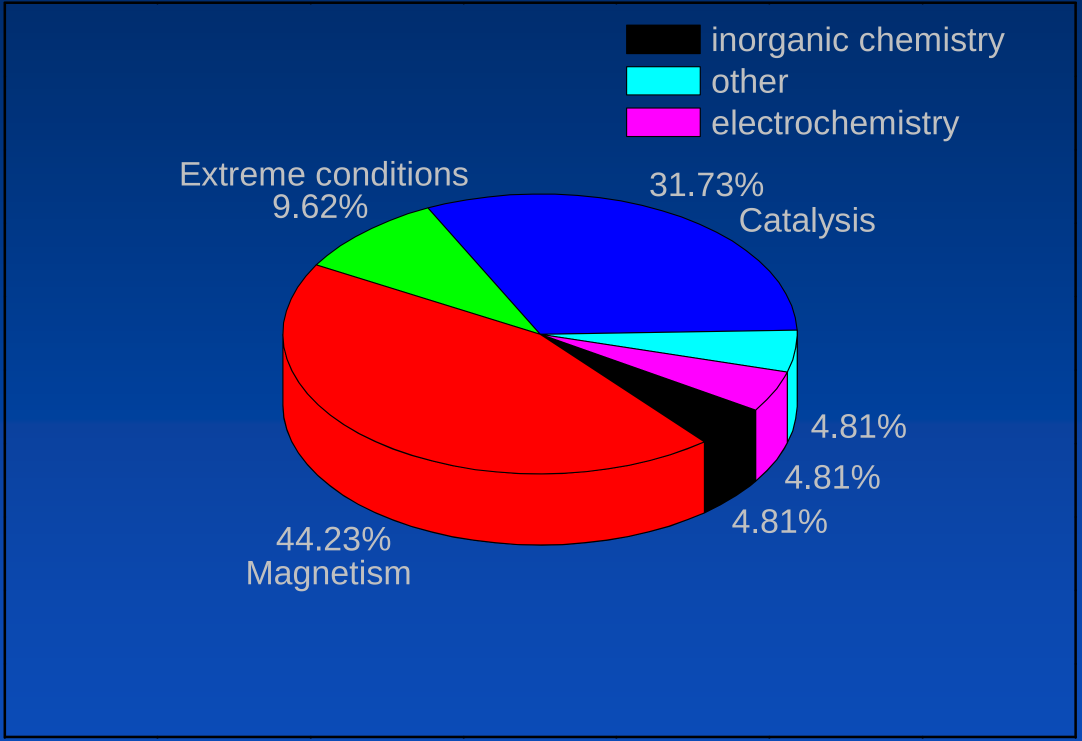

Oversubscribed
25 experiments per year
~10 publications per year

Instrumentation

- Extreme conditions
  - -Pressure (DAC´s)
  - -Magnetic field (up to 6.5 Tesla)
  - -Temperature (10 – 1400K)

- Kinectic studies
  - -Furnaces and reactors (gases/liquids)
  - -Mass spectrometer
  - -Potentiostats & electrochemical cells

6.5T
UHV compatible
Cryo-free

vertical (CF60)
horizontal (CF100)
criostat, furnace, DAC etc...

Cryomagnetics INC.

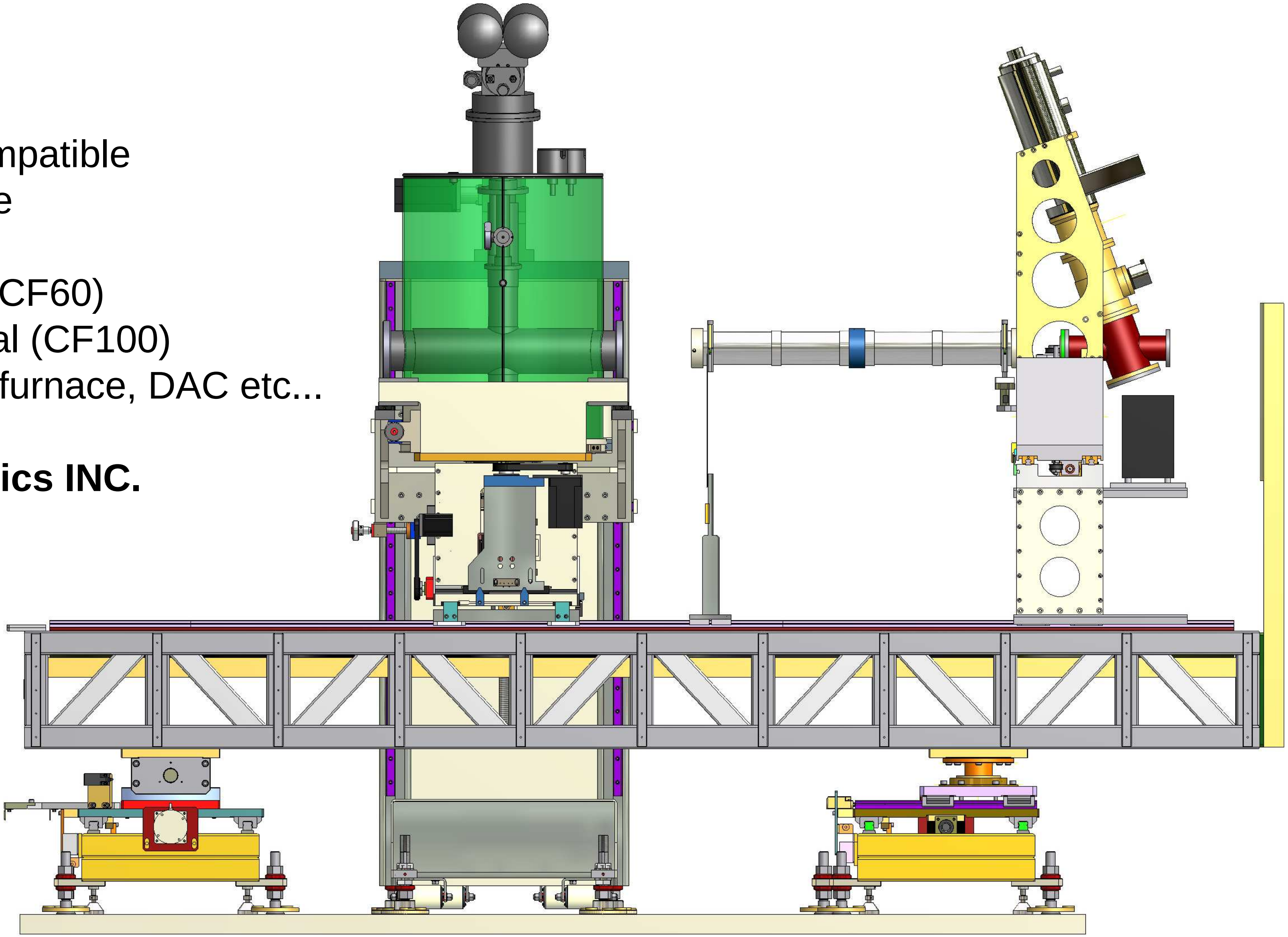

Examples

Formation of NiO nanoparticles monitored in situ by Dispersive XAS

by Meneses et al.

Sol-Gel route to NiO nanoparticle synthesis:

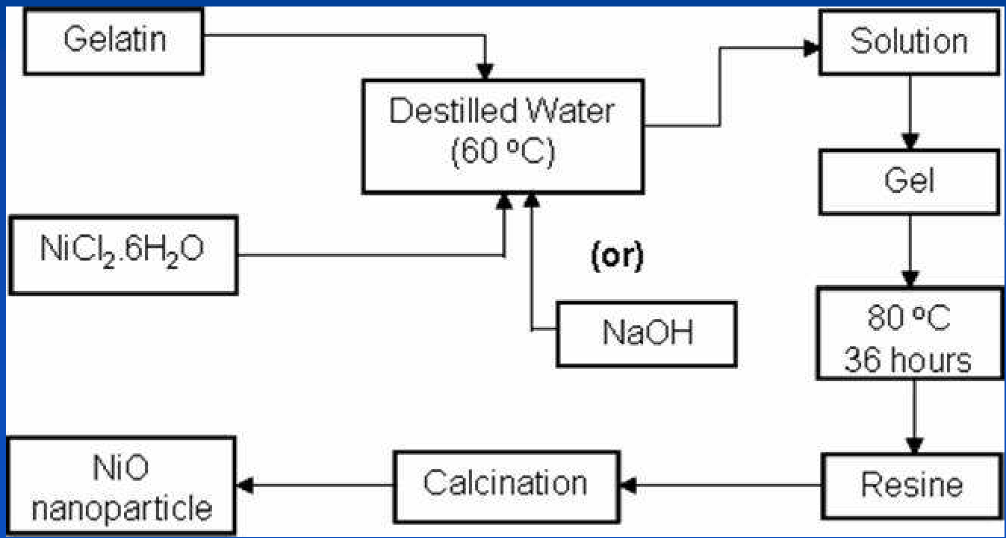

250 <T < 300℃: Ni linked to aminoacids

T > 300℃: amorphous NiO in carbon matrix

C.T. Meseses et al, *J. Nanoparticle Res.* **9**, 501 (2007)

Halogen lamp furnace

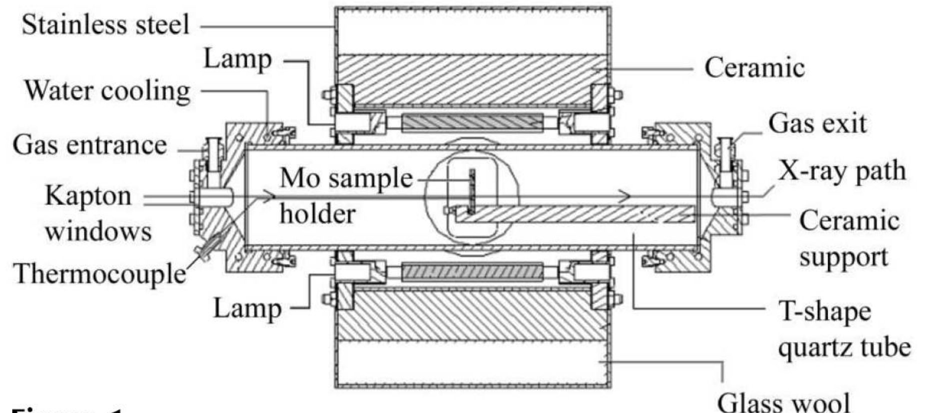

Figure 1
Schematic of the furnace experimental set-up and components.

C T Meneses et al, J. Synchrotron Rad 13, 468 (2006)

12 x 500 W lamps
Temperature range: 200-1000ºC

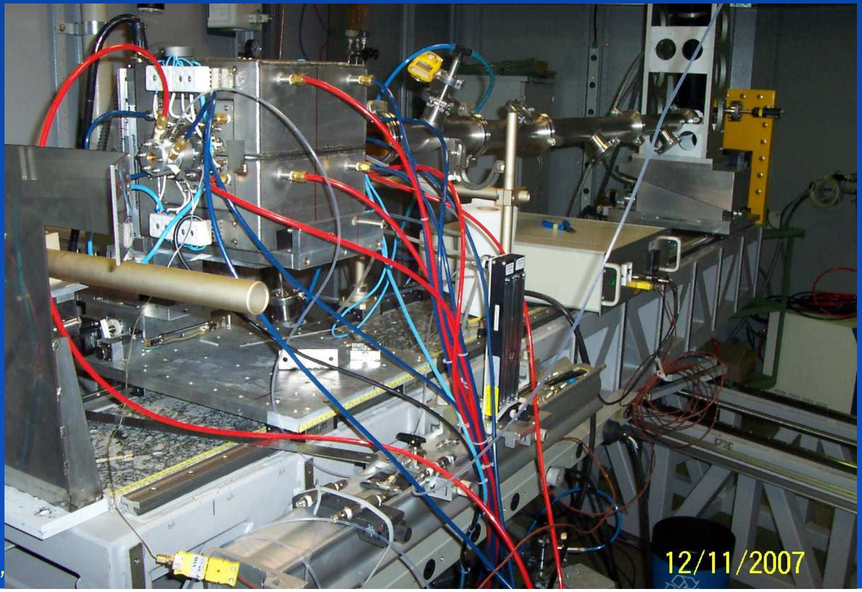

Nanoparticle preparation

- Nucleation process
- Intermediate phases/structures
- Disorder x size
- Size control

Tailored properties

50 x 30 ms frames per spectrum
Heating rate: 5℃/min

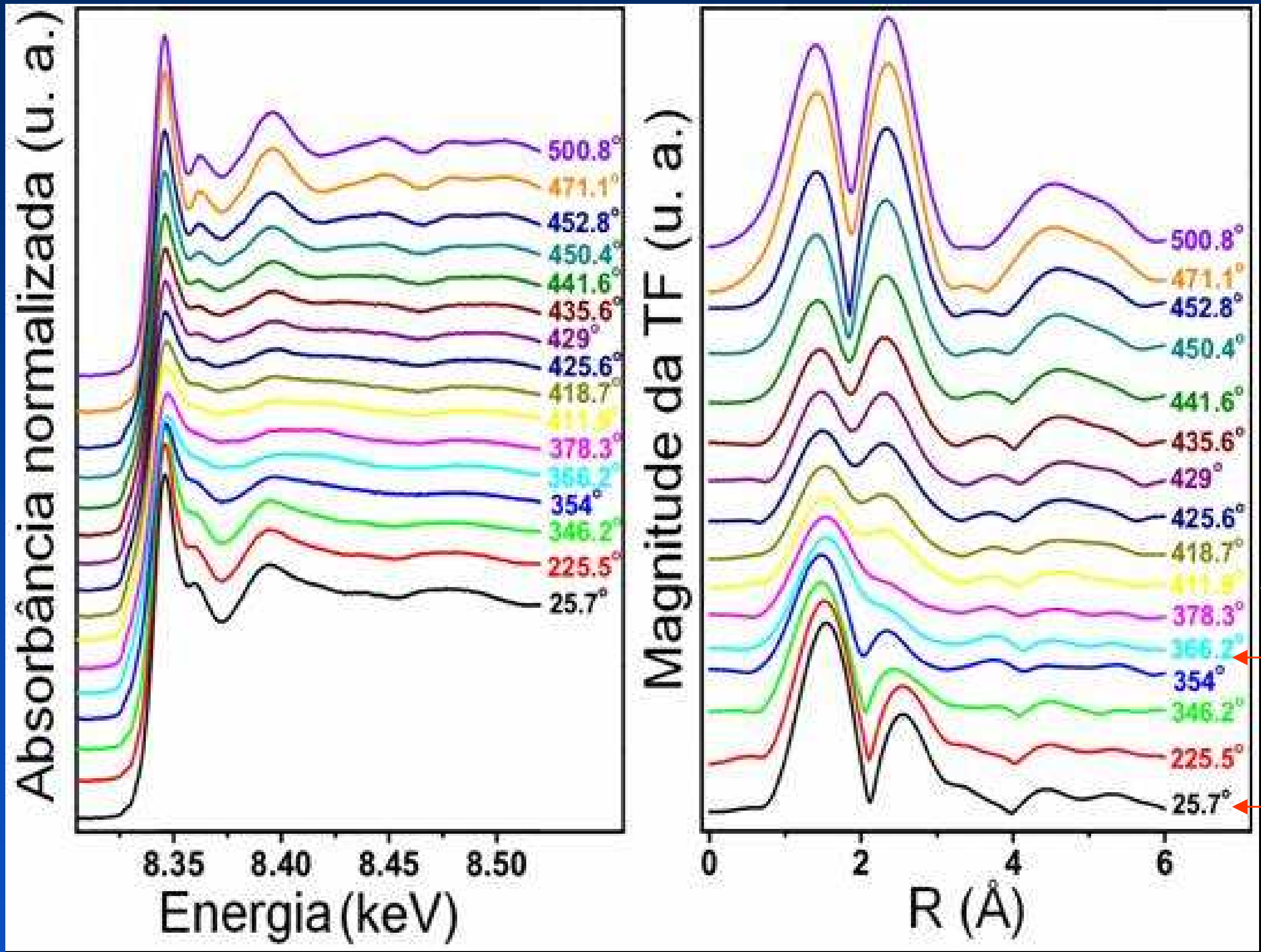

Formation of NiO nanoparticles

Ni dispersed in carbon

$Ni(OH)_2$

Meneses et al, *J. Electron Spec. and Related Phenom*. **156**, 176 (2007)

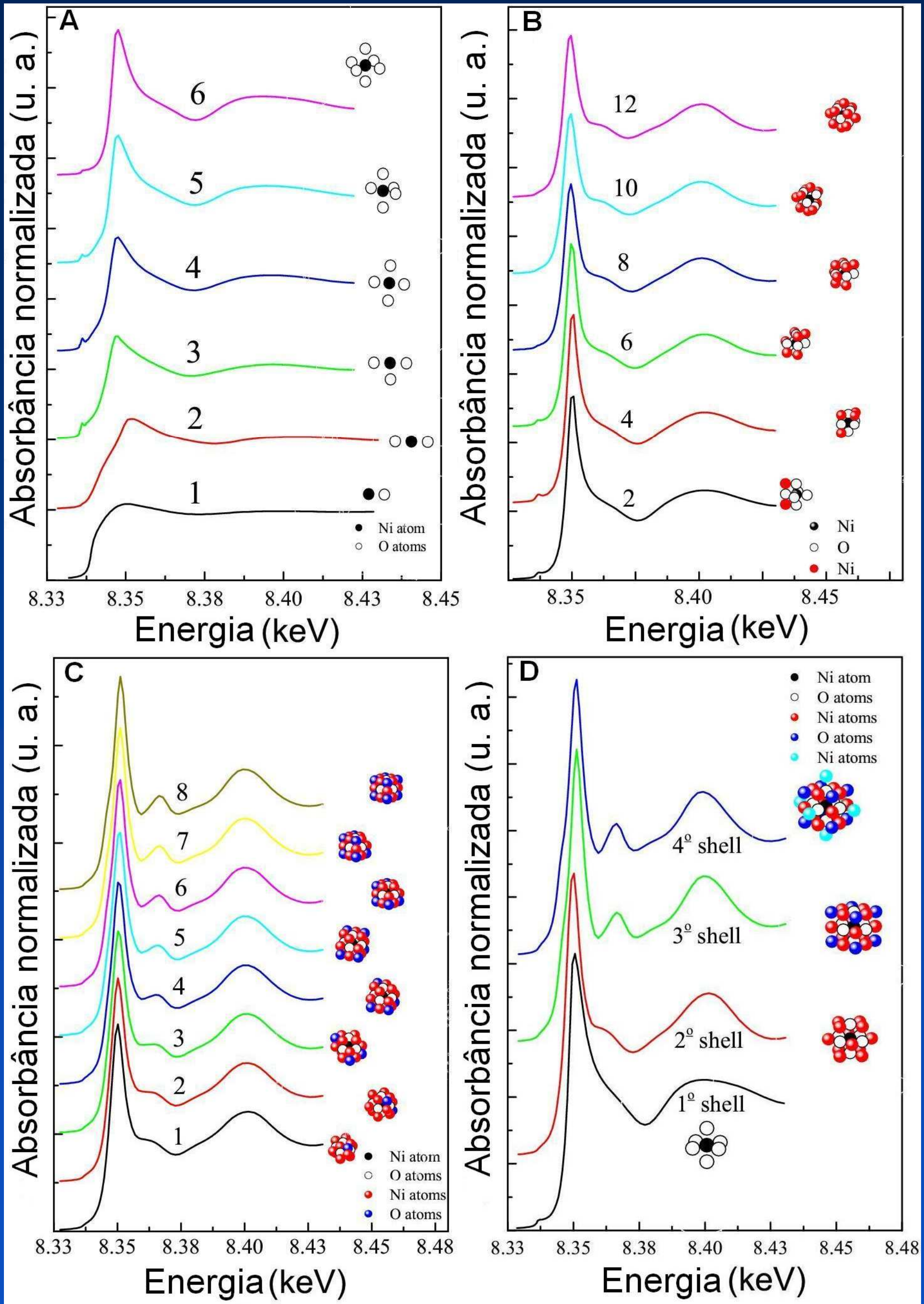

FEFF 8.0 calculations

C. T. Meneses et al
Chem. Materials **19**, 1024 (2007).

Depth-dependent chemical and magnetic properties in nanometric CoPt thin films

by Souza-Netto et al

Analysis of CoPt thin films presenting Perpendicular Magnetic Anisotropy (PMA)

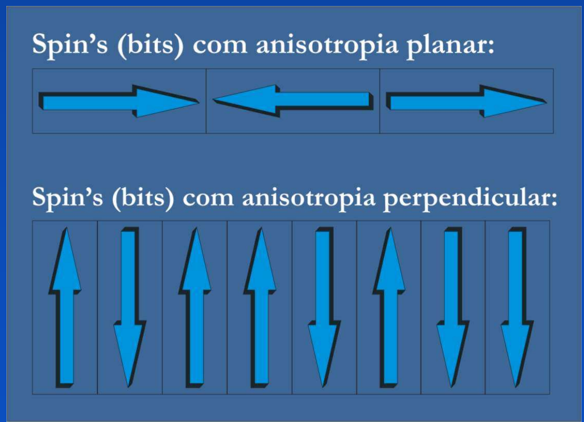

Magnetization results

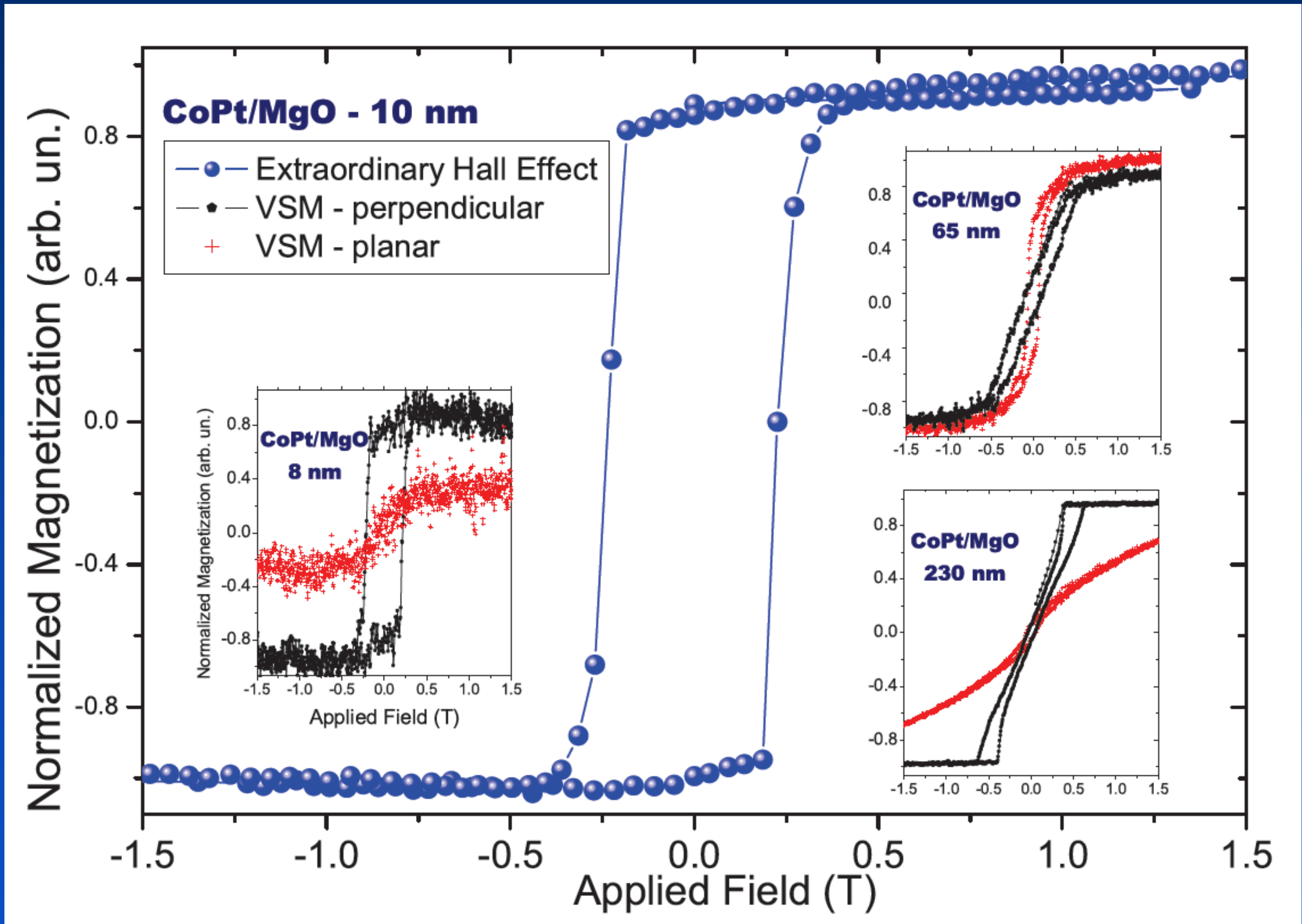

What is the correlation between magnetic and structural properties as a function of sample Thickness?

↓

Grazing Incidence XAS (GIXAS)
Depth-dependent chemica
Magnetic and structural information

Grazing incidence set-up at LNLS beam lines:

XAFS and DXAS

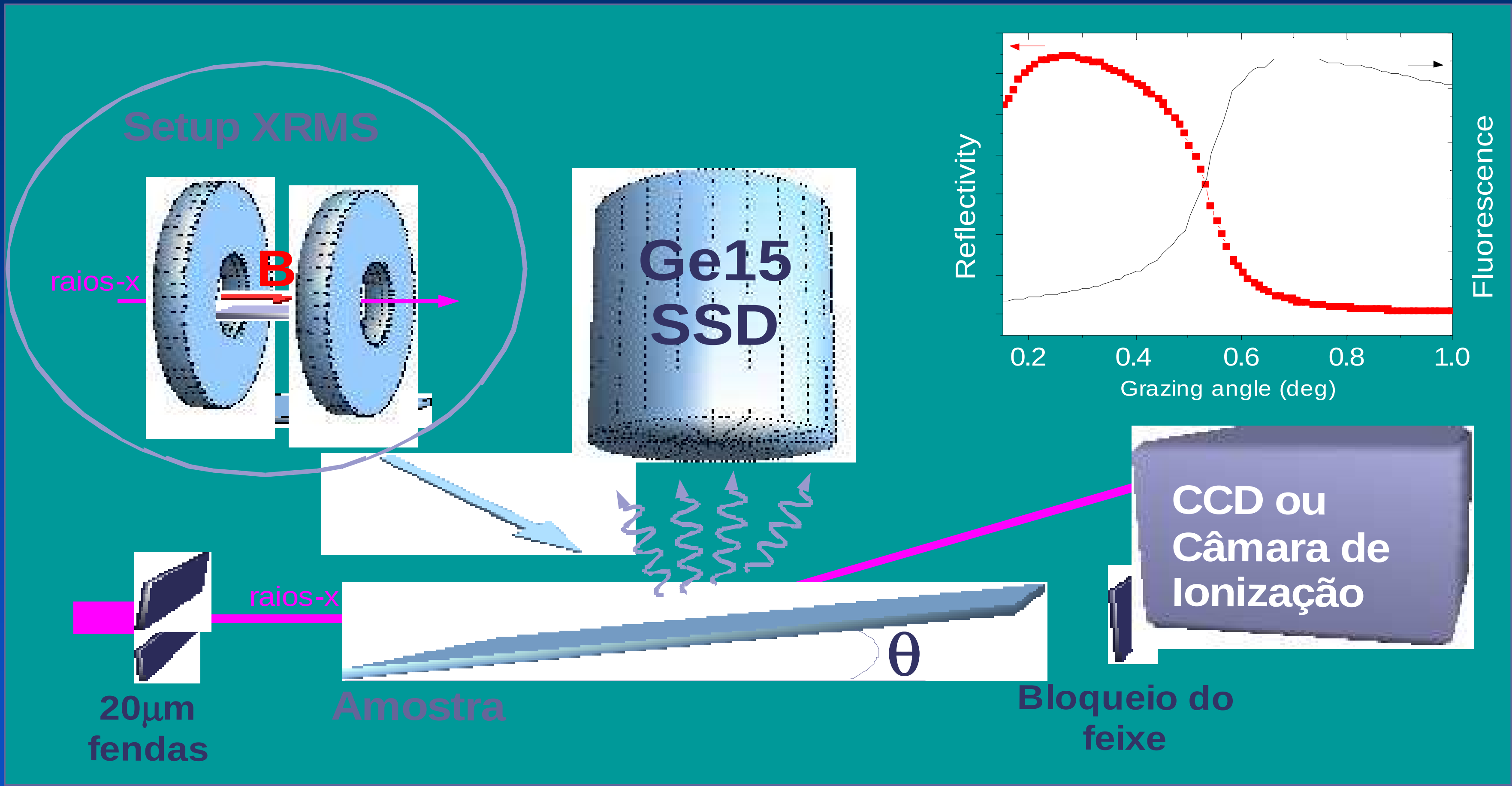

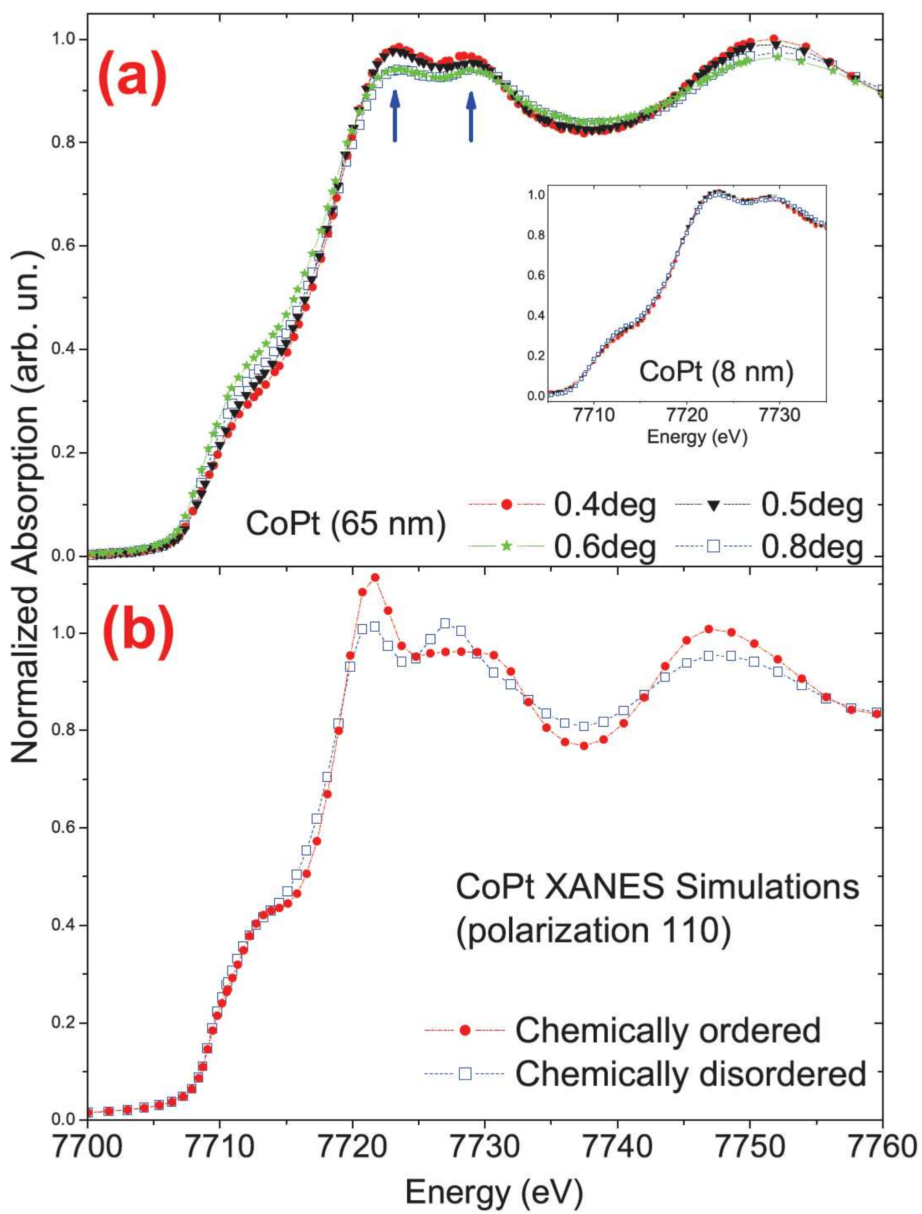

Chemically disordered
FCC

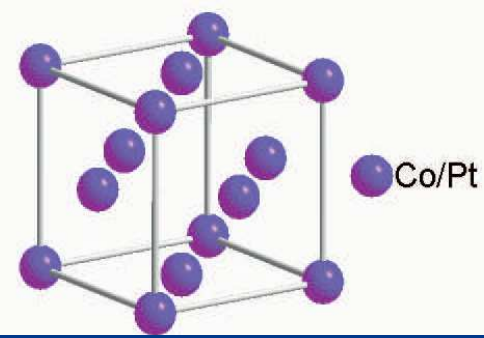

Chemically ordered
FCT

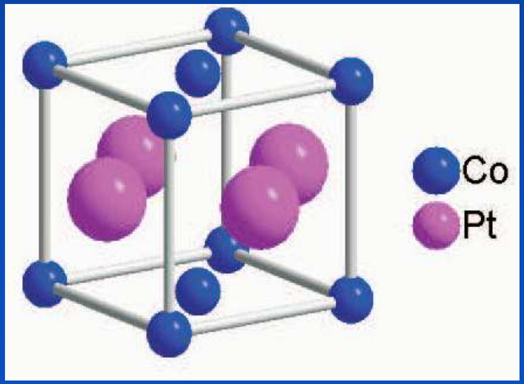

PMA

Souza-Netto et al, *Appl. Phys. Lett* **89**, 111910 (2006)

GIXAS in dispersive mode

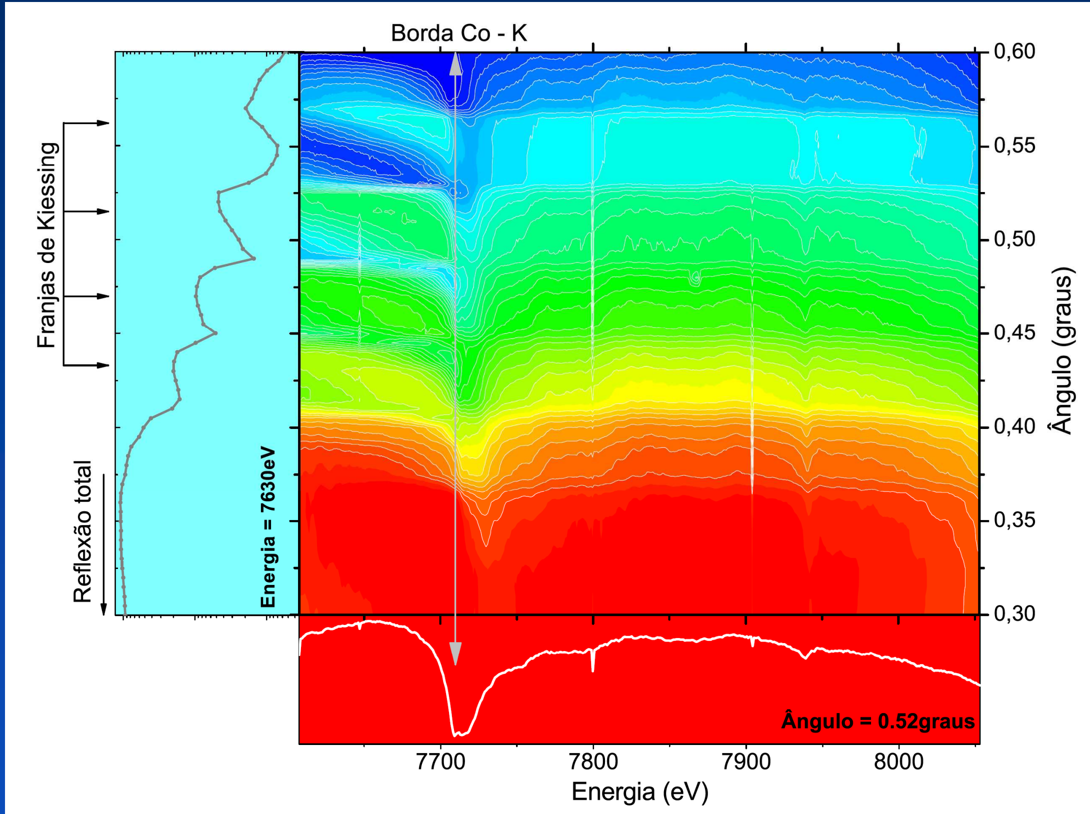

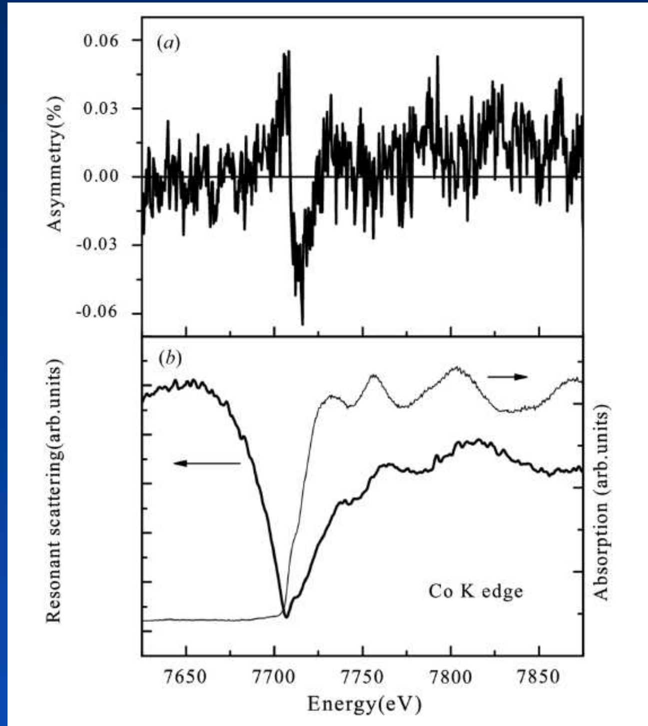

Figure 8
Intensity asymmetry ratio (*a*) and X-ray resonant scattering (*b*) at the Co *K* edge for the multilayer structure $(Co_{1\,nm}/Gd_{0.2\,nm})_{40}$ over SiO_2. The beam of about 70% circularly polarized photons reaches the sample with a grazing angle of 0.49°. The absorption cross section for Co metallic foil in transmission mode is also shown in (*b*).

[Gd0,2 nmCo1 nm]x40 /Si.

Tolentino et al, *J. Synchrotron. Rad* **12**, 168 (2005)

$$R_{XRMS} = \frac{I^+ - I^-}{I^+ + I^-}$$

XRMS

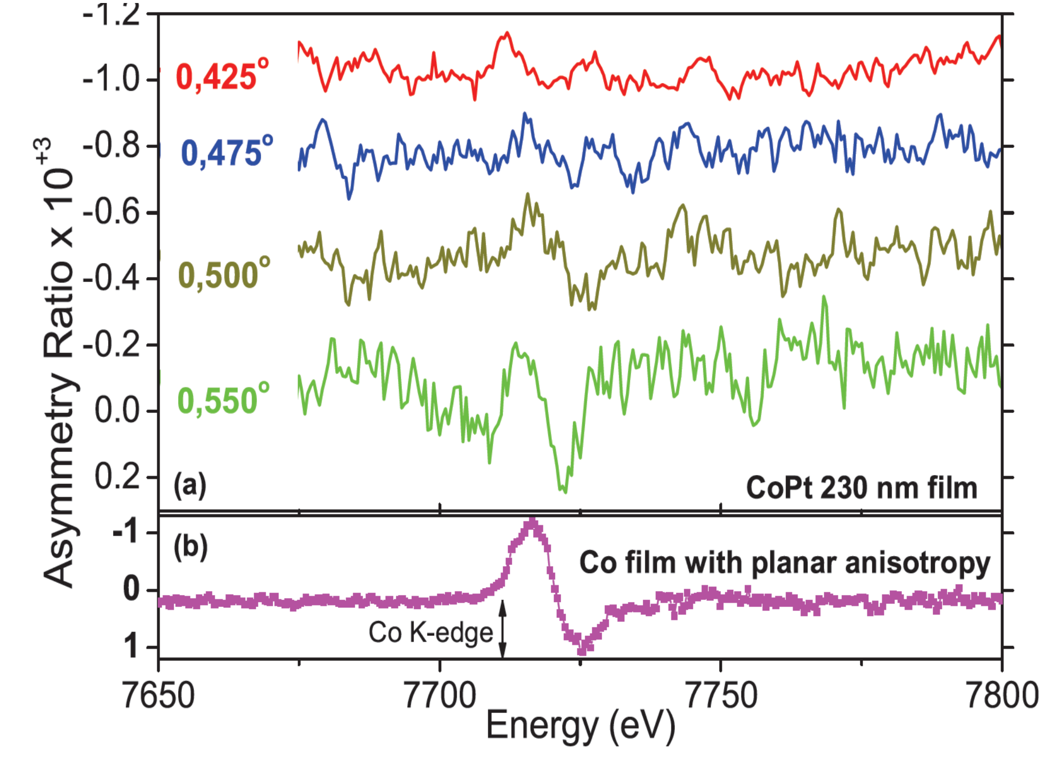

FCT / FCC
Order / Disorder

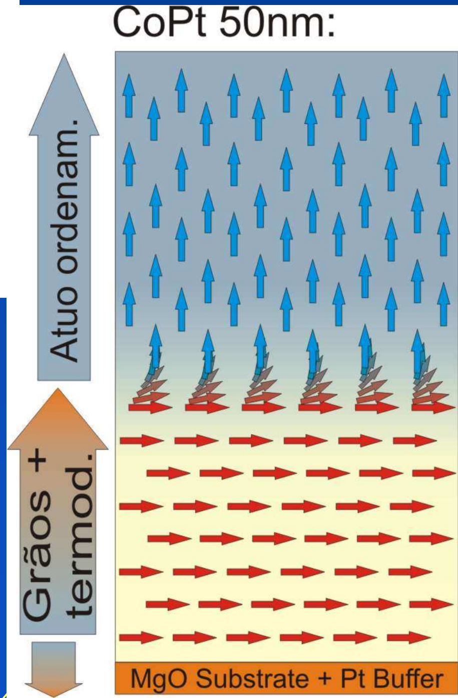

FCT (ordem)

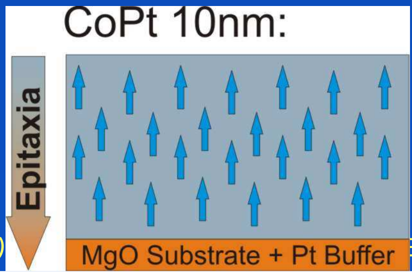

Jahn-Teller distortion in $LaMnO_3$ under pressure

by Ramos et al

$LaMnO_3$

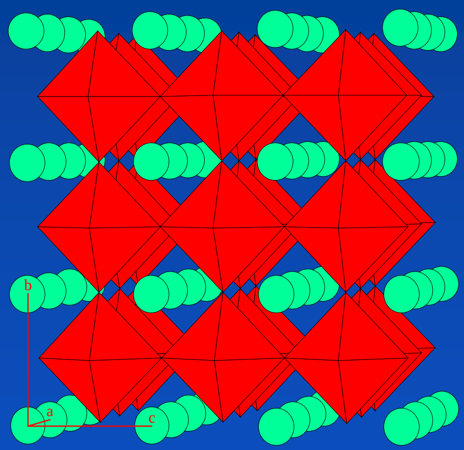

(insulator) Orthorhombic Jahn-Teller → (metal) cubic

~ 730 K (room pressure).
RT (32 GPa)

Theory: JT distortion stabilizes insulating phase

Diffraction: JT distortion quenched above 18 GPa

XAFS as a function of pressure

Dificulty: absorption by diamond anvils

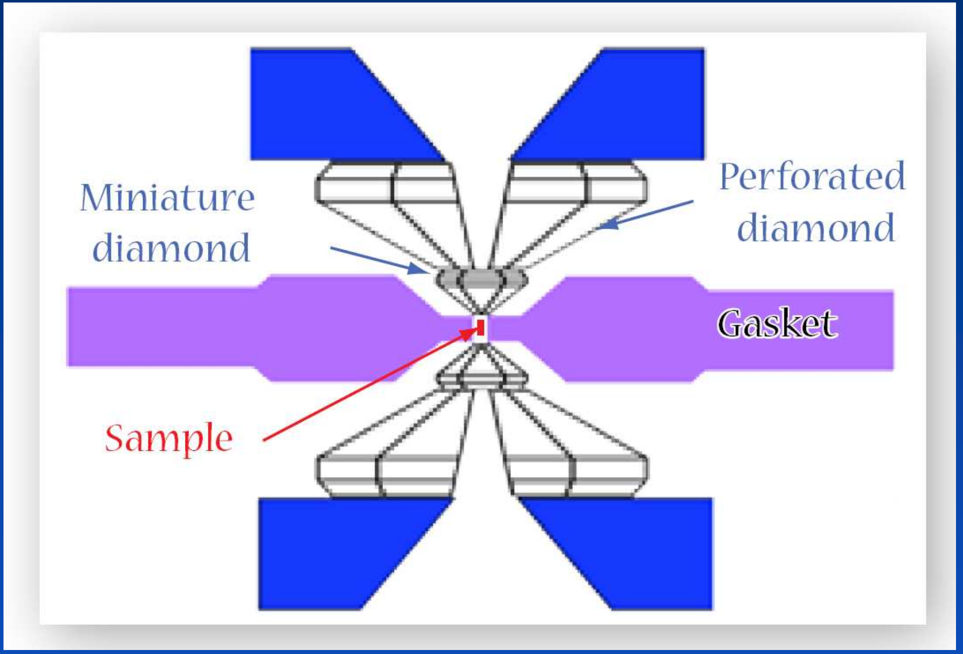

FEFF calculations

A Ramos et al, *Phys. Rev. B* 75, 052103 (2007)

XAFS as a function of pressure

Dificulty: absorption by diamond anvils

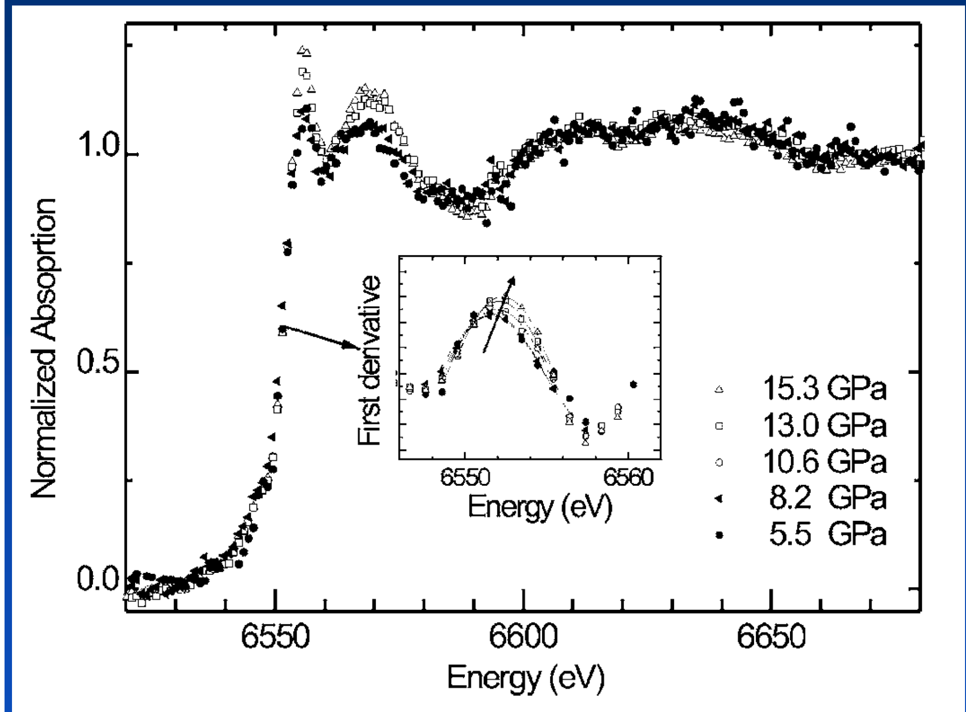

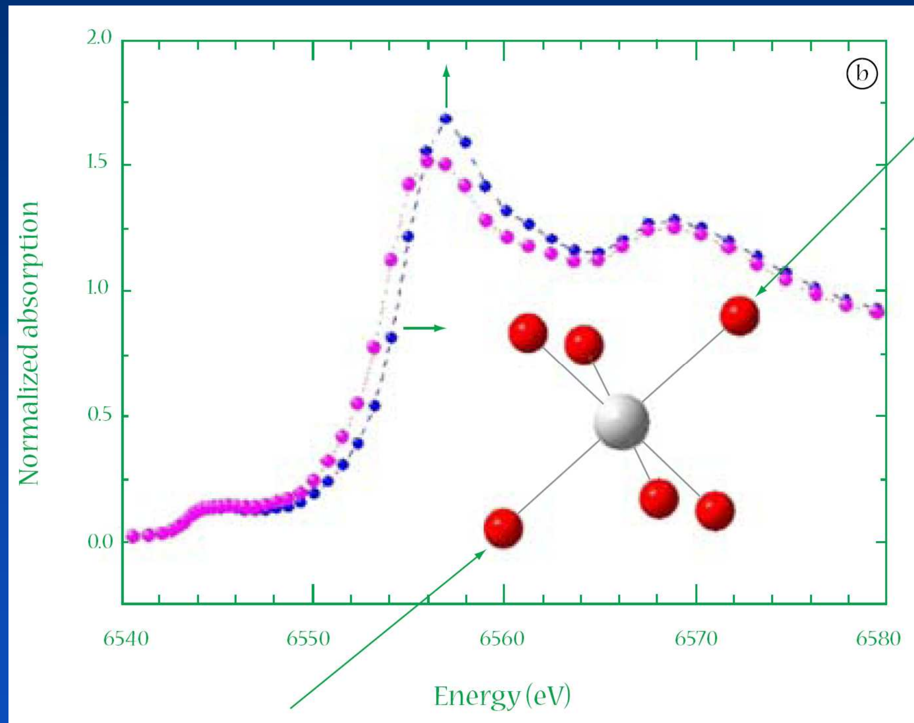

FEFF calculations

A Ramos et al, *Phys. Rev. B* 75, 052103 (2007)

$$\sigma_{JT} = \sqrt{\tfrac{1}{6}\sum \left| R_i - R \right|}$$

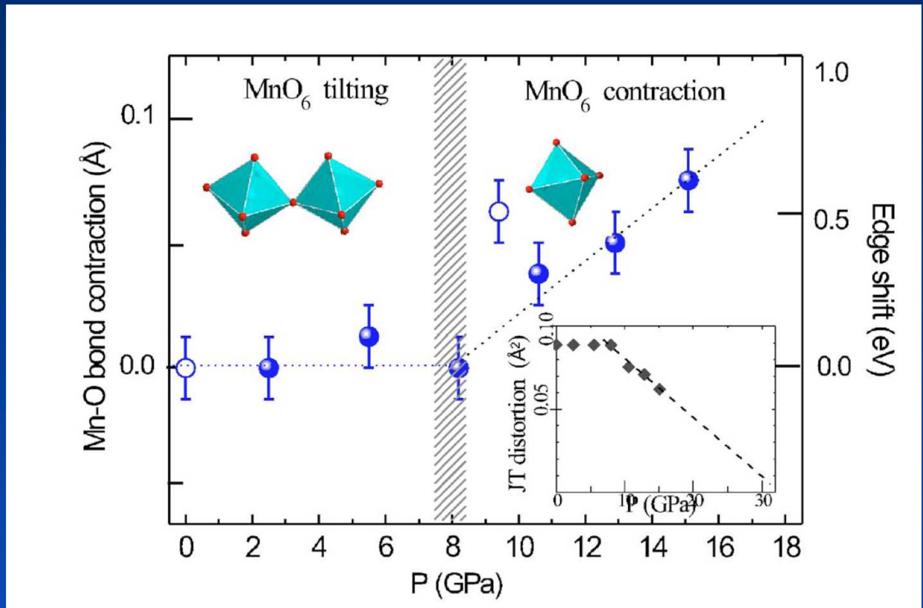

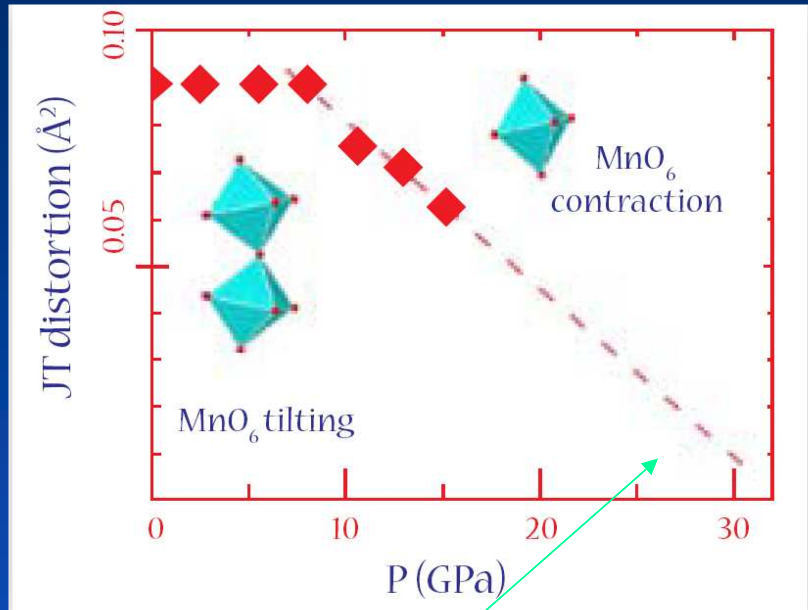

Local JT distortion vanishes above 30 GPa
It is closely related to insulator-to-metal transition

Orbital order in Ba_2FeReO_6

Azimonte et al

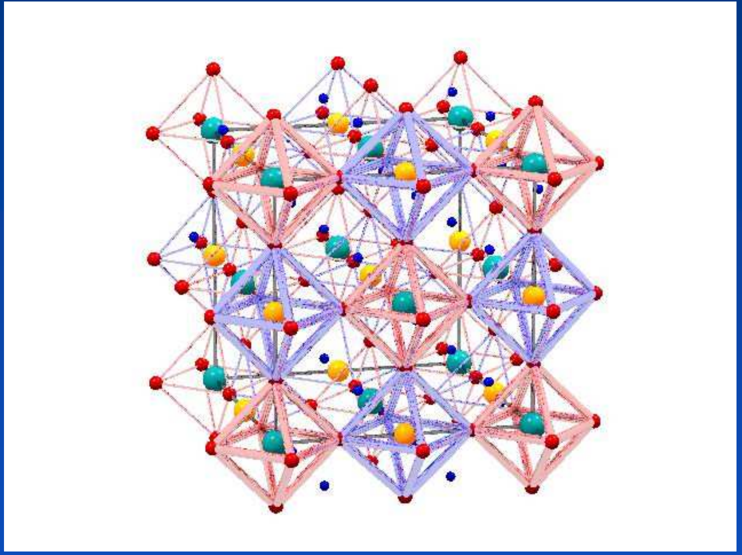

Half-metallic compound (spintronics)

Structure x Magnetism: combination of many techniques
•NPD (Neutron diffraction)
•s-XPD (synchrotron powder diffraction
•XMCD – X-ray absorption

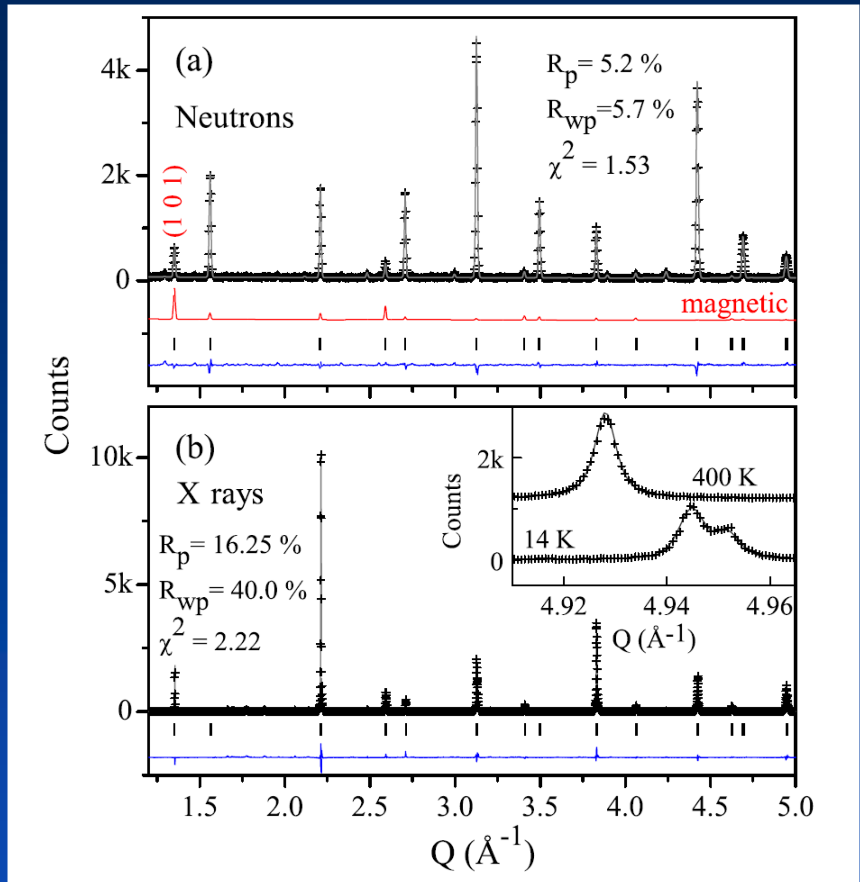

Deviation from Double perovskite Structure:

Tetragonal distortion of the oxygen tetrahedra at low temperatures

Cubic symmetry at high T.

Concomitant magnetic and structural transitions

Tetragonal to cubic perovskite transition
At 309K + Magnetic transition at 304 K

Relative tetragonal distortion

$(\mu(Fe) - \mu(Re))^2$

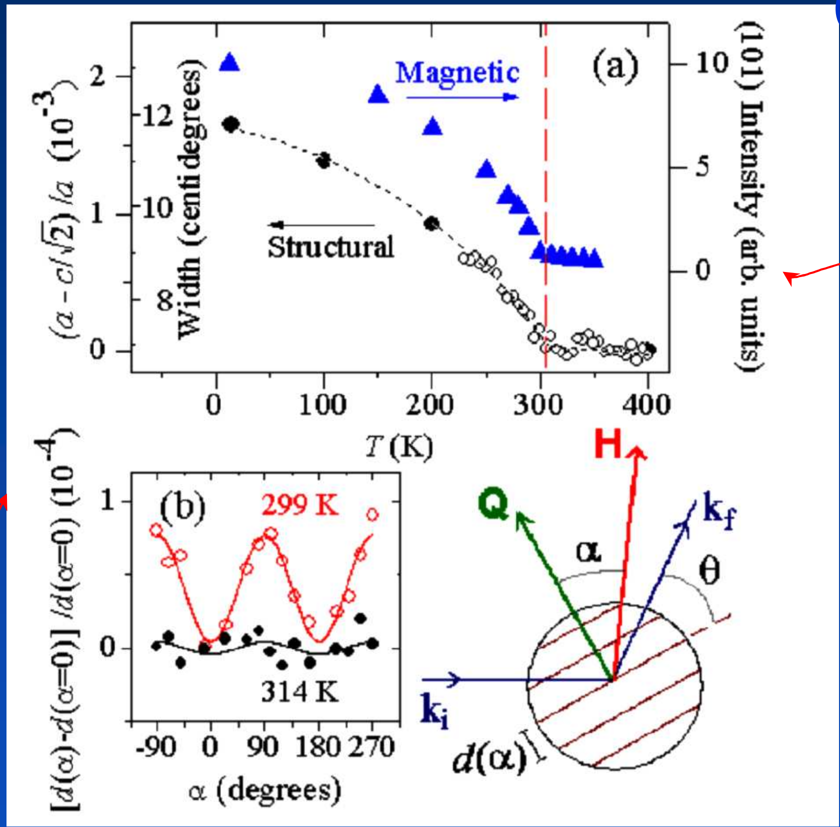

H=0.9 Tesla

Magneto elastic transition – Cryslline structure compressed along the magnetic moment direction

XMCD: Re(DXAS)
Fe(ID08-ESRF)

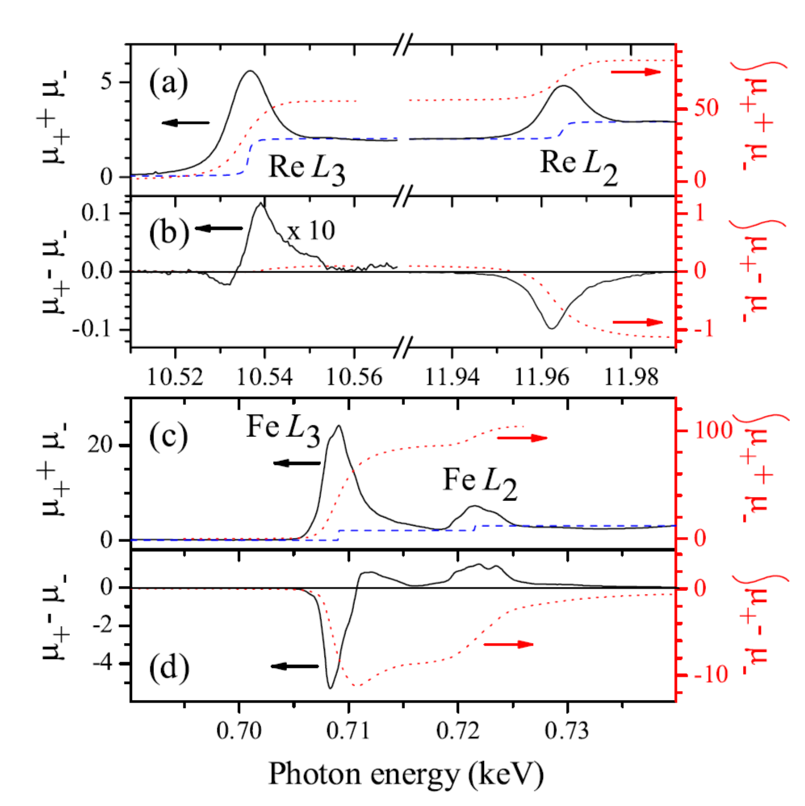

$m_{spin}(Fe) = 2.8(2)\ \mu_B$
$m_{orb}(Fe) = 0.04(2)\ \mu_B$
quenched 3d orbital moments

$m_{spin}(Re) = -0.64(4)\ \mu_B$
$m_{orb}(Re) = 0.19(1)\ \mu_B$
unquenched 5d orbital moments

Strong L.S coupling in
5d Magnetism of Re

XMCD helps understand diffraction data

Re unquenched orbital moments: Symmetry lowering around Re. Cooperative process bellow ordering temperature due to coupling of orbital and spin degrees of freedom, leading to magnetostructural phase transition

Azimonte et al, *Phys. Rev. Lett*. **98** 017204 (2007)